Vol. 44 (2001), 3, 504-508
TRIBOLOGY TRANSACTIONS

Study of the Tribological Behavior of a Thrust Washer Bearing©

ROBERT L. JACKSON (Member, STLE) and ITZHAK GREEN (Fellow, STLE)
Georgia Institute of Technology
George W. Woodruff School of Mechanical Engineering
Atlanta, Georgia

This study addresses the mechanisms that distress a flat-faced thrust washer bearing system. This washer bearing system separates a helical gear and its carrier within a gearset. It was found that the bearing can experience distress by the combination of rotational speed, axial load, and the sequence and rate of their application. Distress is defined as a sudden rise in the real-time frictional torque and temperature.

The various tests suggest the presence of hydrodynamic effects at certain rotational speeds and axial load combinations marked by decreases in the calculated effective coefficient of friction with decreases in velocity. In the tested cases, a distinct increase in the coefficient of friction occurs at the instant of distress.

KEY WORDS

Bearing; Boundary Lubrication; Failure Testing; Failure Analysis; Friction Testing; Helical Gears; Mist and Splash Lubricant Application Methods

INTRODUCTION

The goal of this research is to characterize the conditions that distress the thrust washer bearing system. The thrust washer bearing system consists of two flat-faced washers that are placed between an idle helical gear and its carrier. In some applications, because of non-axisymmetric loading, the gears and washers are tilted in relation to the carrier, forming a converging gap. Because of such tilt, there are sections of contact between the components. From this point forward, "bearing" will refer to the thrust washer bearing system within the test rig, unless specified otherwise.

The bearing must bear the load produced by an idle gear of a helical gearset. A gear considered idle transfers no torque to the shaft it rides on. The axial load placed on the thrust washer is induced by a combination of helical gear forces and forces induced by the skewing of the needles upon which the gear rides. Skewing of these needles could be the cause of additional axial thrust loads; this problem has been studied by Ulezelski, et al. (1983), and experimentally confirmed by Bair and Winer (1989).

Other research has looked into certain aspects of the bearing behavior, but not the behavior of the system as a whole. For instance, Shamim (1994) investigated the effectiveness of mist lubrication in machinery, and found that it works well in some cases. It is believed that the lubrication on and around the washer and gears is a mist produced by the squirting of fluid and the splashing of the gears.

Taniguchi and Ettles (1973) performed an experimental and theoretical analysis of a thrust washer bearing, although the thrust washer used had radial grooves and no tilt. They do state generally that washers with increased random waviness perform better. McClintlock (1974) also performed an experimental investigation of a similar bearing. However, he claims that roughness can cause additional washer wear.

To gain an understanding of the thrust washer bearing behavior under non-axisymmetric loading, a test rig was designed to provide a physical model. The test rig allows controlled variation in the operational parameters governing the tribological behavior of the washer. For given washer materials and surface finishes, the parameters that most affect the life of the bearing and its tribological behavior are believed to be thrust or axial load, rotational speed, lubrication supply, lubrication properties, and the geometry of the bearing.

The test rig also records pertinent real-time data from the bearing. For the initial phase of testing it seemed logical to monitor two real-time indicators of bearing behavior: the frictional torque transferred through the bearing and the temperature near the bearing.

Presented at the 56th Annual Meeting
Orlando, Florida
May 20-24, 2001
Final manuscript approved June 7, 2001
Review led by Greg Kostrzewsky

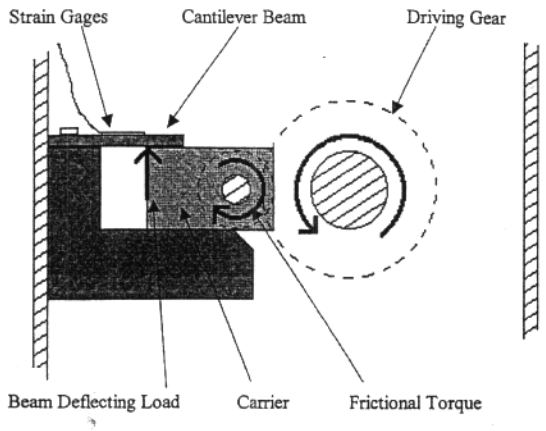

Fig. 1—Diagram of the test rig at the thrust washer-bearing interface.

TEST RIG

An electric motor is used to drive a shaft, which drives the larger gear, which in turn drives the smaller gear. The pinion and bearings are loaded by a press attached to a lever, which is loaded by a cable that exits the rig and follows a series of pulleys to a hanger. The hanger can be loaded with an assortment of weights and thus impose various axial loads on the bearing. The pinion rides on a series of needles (forming a needle bearing) placed between the shaft and boring. A steel gearbox encloses the gears, loading system, and lubricant.

Taking advantage of the gear speed ratio, the driven gear can be rotated at a maximum rotational speed approximately twice that of the powering motor. The motor is controlled by an inverter unit, which is digitally programmed by a PC.

In the test rig a majority of the axial load is induced by a lever pressing from one side of the gear and bearing assembly. In practice, the bearings are loaded by the axial forces of the meshing of helical gear teeth and the skewing of the needle bearing upon which the gear rides. In the test rig the axial load is applied using a tapered face to cause a tilt of the pinion to simulate the actual non-axisymmetric loading conditions. It is believed, however, that on a qualitative and comparative basis the results from this test rig can be useful in determining the distressing conditions seen in practice.

Since the gears used are helical in the test rig, an additional load is also applied to the bearing. The force is directly related to the torque. This force is very small in comparison to the manually applied axial load and so is not taken into account. Since no significant load causes the needles between the gear and shaft to skew, the load induced by the skewing is ignored.

A torque sensor was designed and fabricated to record the torque transferred through the bearing and onto the carrier. The torque transferred through the bearing is directly related to the effective coefficient of friction, since friction is the mechanism that transfers torque from the bearing to the carrier. As with most bearings, it is desired that the coefficient of friction be as small as possible to minimize the generation of thermal energy. The friction does not only represent energy loss, but can also be related to wear, because when a bearing wears its friction will be higher, since energy is lost in removing material from the bearing.

A cantilever beam measures the torque transferred through the bearing, which bends as the torque turns the bearing carrier (see Fig. 1). As the torque transferred through friction from the washers to the carrier increases, the carrier is forced to rotate. The cantilever beam then absorbs this torque by bending. Strain gages adhered to the beam then bend with the beam. Thus, the amount of strain of the gages is proportional to the frictional torque.

Thermocouples indicate the temperature near the bearing. Four thermocouples are embedded in the stationary carrier next to the bearing. Another thermocouple placed at the bottom of a plate positioned directly below the bearing gathers the exiting lubrication and reads its temperature.

All the sensors are wired into a data acquisition system, which amplifies and filters the signals before they are acquired by a data acquisition board installed in a PC. Professional software is used to record and plot the data in real-time.

A lubrication system is also provided to lubricate the tested bearing and also the other bearings used in the test rig. A flow meter measures the fluid flow to the bearing. In the test rig the lubrication system can supply lubrication at a variety of flow rates. A gear pump is used to pressurize the fluid, thus causing it to flow into lubrication applicators within the gearbox. A filter, placed ahead of the pump, removes any significant debris that might affect the gear pump and the thrust bearing performance. The inside of the gearbox acts as an oil sump from which the lubrication is cycled.

The applicators expel lubrication to the thrust washer bearing from above. The applicator consists of a pressurized cylinder through which lubrication enters from the outside of the gearbox. The lubricant then exits through a small hole pointed towards the bearing.

EXPERIMENTAL METHODOLOGY

All values have been non-dimensionalized for generality. For each loading condition a non-dimensional PV (pressure•velocity product) value is calculated using the following equation:

$$PV = \frac{N \cdot F_a}{N_{max} \cdot F_{max}} \qquad [1]$$

where

N - rotational speed, [rps]
F_a - axial load, [N]
N_{max} - maximum tested rotational speed, [rps]
F_{max} - maximum tested axial load, [N]

The PV value is meant to represent the total tribological "stress" the bearing is under. In other words, the effectiveness of the bearing can be quantified by how high a PV value the bearing can sustain without distress or significant friction. Distress is defined as a point when the temperature or frictional torque rises suddenly.

An experimental model of the bearing at different loads, speeds, or different PV values is desired. During these tests the lubrication flow rate is kept constant at the maximum rate. Three

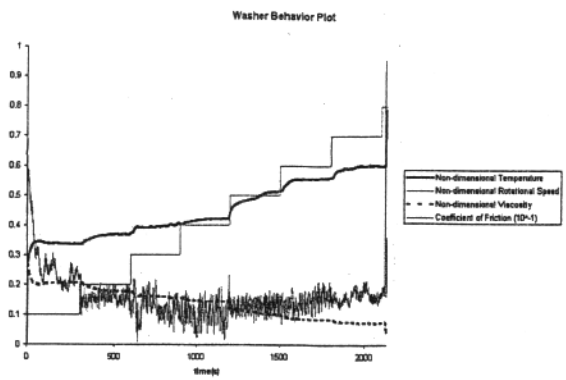

Fig. 2—Sample plot of test rig data. Velocity is incremented from low to high speeds. The load is held constant.

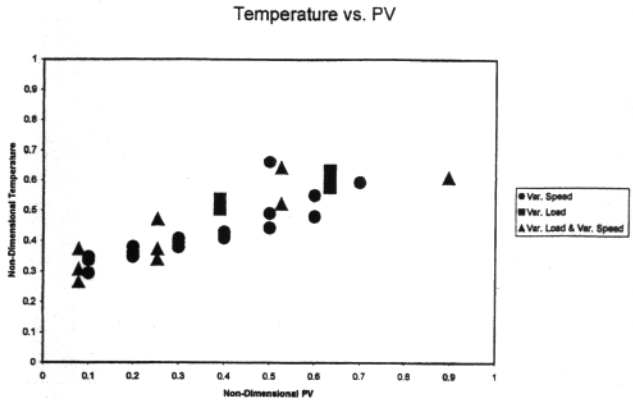

Fig. 3—Plot of temperature data from all tests *vs.* pressure-velocity value.

types of tests are thus used to obtain data:

1. The rotational speed is kept constant while the axial load is increased in steps until distress is achieved.
2. The axial load is kept constant while the rotational speed is increased in steps until distress is achieved.
3. Both the axial load and rotational speed are increased simultaneously until distress is achieved.

Each step is incrementally increased at the same intervals for each test type. These intervals were obtained from previous tests by observing how long it took the bearing to reach a near steady-state condition. The time increments were then made to be longer.

EXPERIMENTAL RESULTS AND DISCUSSION

The experiments described previously were performed, and all real-time data was recorded. The data was then plotted and analyzed. See Fig. 2 for a sample plot of recorded data. The number of tests conducted does not allow for a meaningful statistical analysis. Therefore, these results are to be considered qualitatively rather than quantitatively.

In these tests the load steps are clearly represented, as is the frictional torque and temperature. A sudden rise in bearing temperature and frictional torque also indicates a clear distress point. In the sample plot it should also be noted that the changes in the friction coefficient usually precede the changes in viscosity. In other words, the viscosity changes do not seem to be causing the changes in the friction; rather the heat dissipated by the friction seems to change the viscosity. At higher speeds more energy must be dissipated by friction even if the friction coefficient is lower, so the temperature often rises even though the friction coefficient is lower.

There is a definite variation in the distress point and behavior within like tests. These variations could be due to manufactured differences in the surface roughness or composition of the bearings. This may also be due to the wearing of those parts used in the test rig that are not replaced between tests or to some variation in the testing procedure that may have affected the bearing behavior. In addition, the same lubricant was used through all the tests and so the lubricant properties may have been altered during testing and thus affected the bearing behavior. A simple analysis of the lubricant viscosity has been performed and demonstrates that viscosity does not change significantly for the number of tests performed.

Steady-State Values

Using the steady-state data from the recorded data sets, the fluid temperature *vs.* PV are plotted in Fig. 3. These plots use the steady-state values at the end of each load step for each value of PV induced during each test. To calculate the torque, an average value is used over the last data points taken for each step of PV. This plot is created in an attempt to find some correlation between the PV value and the bearing behavior. This correlation could then be applied to future tests, especially if accelerated testing is implemented.

As seen in the plot in Fig. 3, the bearing temperatures generally rise with PV. This rise in temperature is expected, since the load induced on the bearing increases, and thus the frictional energy dissipated increases as well. An increase in speed should also increase the temperature since more energy must be dissipated by the bearing.

Effective Coefficient of Friction

Next, the steady-state torque is used to calculate the effective coefficient of friction (COF) for the bearing at the various loaded values of PV (see Figs. 4 and 5). The Appendix contains a short derivation of the formula used in calculating the effective coefficient of friction. This formula is for a surface that is loaded by an even axi-symmetric pressure distribution, even though this is not the tested condition. The formula is given below:

$$\mu = \frac{3}{2} \cdot \frac{T_c\left(r_o^2 - r_i^2\right)}{F_a\left(r_o^3 - r_i^3\right)} \qquad [2]$$

where

μ - effective coefficient of friction
F_a - axial load, [N]
T_c - frictional torque, [N•m]
r_i - inner diameter of washer, [m]
r_o - outer diameter of washer, [m]

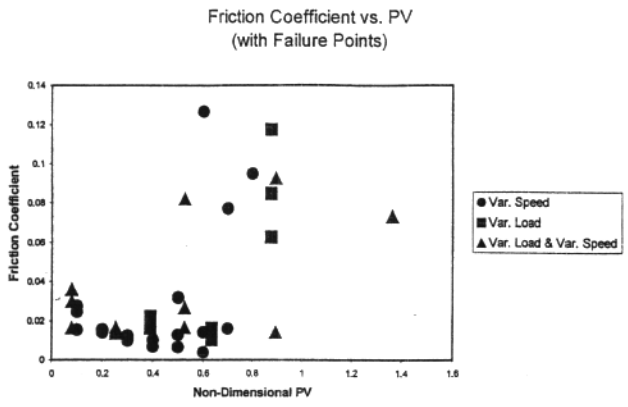

Fig. 4—Plot of steady-state effective coefficient of friction *vs.* pressure-velocity value.

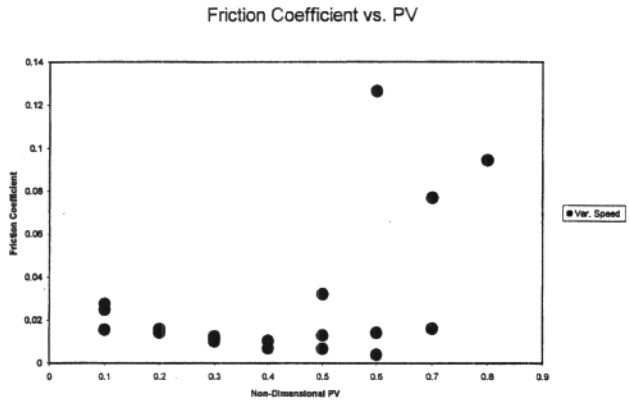

Fig. 5—Plot of steady-state effective coefficient of friction for data from test type 2 (varying speed and constant load).

During operation, the COF varies between 0.004 and 0.13. While the bearing seems to be operating with some indication of hydrodynamic effects, in boundary layer form, mixed lubrication form or full fluid film form, the COF is between 0.004 and 0.036. At the distress points, the COF rises to be between 0.06 and 0.13.

Each calculated COF was plotted *vs.* PV. This plot is presented in Fig. 4. Note that the PV value does not seem to represent the data well, because there does not seem to be a strong trend or pattern.

Although there is some variation in the values of the COF at each PV value (due to various ratios of speed to load), the general trend is that the COF decreases with increasing PV values. Hydrodynamic effects that increase proportionally with the rotational speed or decreasing fluid viscosity probably cause this trend.

If the values for the varied speed (Test Type 2) tests are presented alone the possibility of hydrodynamic lubrication becomes more apparent. Figure 5 shows the varied speed tests plotted alone against PV. Since load does not change, this graph is the same as a plot of the COF *vs.* speed. These results contain some of the highest relative COF seen during these tests at the beginning load steps. This is because at these load steps the rotational speed is low and thus unable to produce any hydrodynamic effects. As the speed is increased though, the COF lowers until bearing distress is reached. Distress at high speeds could be the result of centrifugal effects reaching significance (Pinkus, et al., 1981).

The COF does vary between each individual test of the same conditions for unknown reasons. Perhaps manufacturing inconsistencies in the surface topology or material composition cause these variations. For all three tests though, the COF rises significantly at the distress point, which would suggest dry contact or loss of hydrodynamic effects.

Stribeck Curve

Since the Pressure-Velocity (PV) value did not produce strong trends when it was plotted versus the steady-state coefficient of friction, a different approach was taken. A Stribeck curve is a plot of the coefficient of friction *vs.* the product of the bearing linear speed and viscosity normalized by the average bearing pressure. In equation form this relation is:

$$\mu = \mu\left(\frac{ZN}{P}\right) \qquad [3]$$

where:

μ - coefficient of friction
Z - dynamic viscosity of fluid ($N \cdot s/m^2$)
N - rotational speed (rev/s)
P - average bearing pressure (N/m^2)

This curve is frequently used to qualitatively identify the transitions from boundary lubrication to mixed lubrication, and to hydrodynamic lubrication. When the Stribeck value was used to plot the data from the three types of tests performed, the plot in Fig. 6 resulted.

The data seems to roughly represent the two sides of the Stribeck curve. On the left side of the curve the coefficient of friction is decreasing as the Stribeck value increases. Since these data points were obtained when the bearing speed is varied, the plot suggests that the bearing behavior here is boundary lubrication or on the verge of full film hydrodynamic lubrications. Here hydrodynamic effects cause less friction with increasing speed. On the right side of the curve, the coefficient of friction begins to increase with increasing Stribeck values. These points are supplied by the variable load test, which were run at a very high speed. Thus, the hydrodynamic effect here seems to already be in the full film regime at these speeds.

CONCLUSIONS

Distress of the bearing is linked to load and speed. Both temperature and torque seem to be good indicators of failure, since both increase noticeably at a distress point, although temperature seems to be the better indicator.

The data sets also indicate the possible presence of hydrodynamic effects produced by the bearing at certain combinations of rotational speed and axial load. This is indicated by a decrease in friction with speed, while the temperature and viscosity remain momentarily unchanged (Figs. 2 and 5). When the coefficient of friction is plotted versus the Stribeck value, a trend similar to the

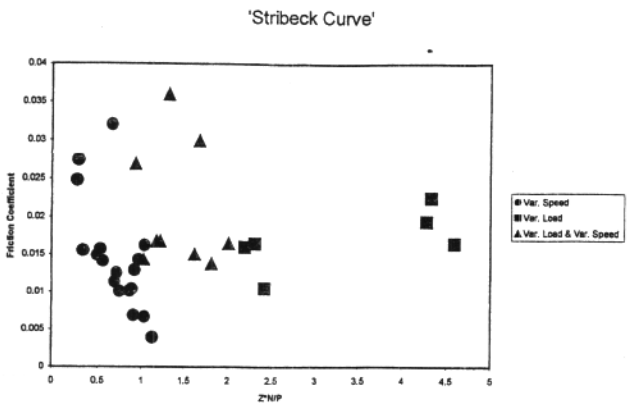

Fig. 6—Plot of calculated effective coefficient of friction using the Stribeck value.

Stribeck Curve is produced. This would suggest that the bearing might be behaving under the influence of boundary layer, elasto-hydrodynamic and hydrodynamic effects.

Due to the coefficient of friction values and the geometry of the bearing, it is believed that these effects are caused by a thin boundary layer at the contact point and possibly a full film at higher speeds. It has been shown in past works that the coefficient of friction indicates various lubrication conditions (Hamrock, 1994). Thus, the COF indicates the bearing behavior as it traverses between the most desirable hydrodynamic lubrication through elasto-hydrodynamic, boundary and also unlubricated contact, although all conditions may not be represented. At a distress point seen in all the tests, however, the COF increases sharply and is believed to represent a fluid film breakdown.

Due to the number of tests conducted, these results are regarded qualitatively rather than quantitatively. In the future, additional tests will have to be performed for a statistical analysis to be possible.

ACKNOWLEDGMENTS

This research was funded by General Motors through the Center for Surface Engineering and Tribology. Mr. David Stark and Mr. David Zini are the program managers. This support is gratefully acknowledged.

REFERENCES

(1) Bair, S. and Winer, W. O., "Tribological Characteristics of Needle Bearings," in Proc. Leeds-Lyon Symp., (1989).

(2) Hamrock, B. J., *Fundamentals of Fluid Film Lubrication*, NY, McGraw-Hill, p 8, (1994).

(3) McClintlock, R., "A Laboratory Study of Automatic Transmission Thrust Washer Wear," SAE Preprint **740050**, (1974).

(4) Pinkus, O. and Lund, J. W., "Centrifugal Effects in Thrust Bearings and Seal Under Laminar Conditions," *Trans. of ASME*, **103**, pp 126-136, (1981).

(5) Shamim, A. and Kettleborough, C. F., "Tribological Performance Evaluation of Oil Mist Lubrication," *Trans. of ASME*, **116**, pp 224-231, (1994).

(6) Taniguchi, S. and Ettles, C., "A Thermo-Elastic Analysis of the Parallel Surface Thrust Washer," *ASLE Trans.*, **16**, pp 299-305, (1975).

(7) Ulezelski, J. C., Evans, D. G., Haka, R. J. and Malloy, J. D., "Needle Bearing Axial Thrust Study," SAE Technical Paper Series, **830568**, (1983).

APPENDIX

Derivation of the Coefficient of Friction for an Axisymmetric Geometry and an Evenly Distributed Load

For an annulus of inner radius, r_o, and outer radius, r_i, an infinitesimally small portion of the bearing surface has an area dA. The normal force on the surface is then given by the formula:

$$dN=PdA \qquad [A1]$$

where P is the evenly distributed pressure and dN is the normal force. The friction force, df, applied to the area is then given by

$$df=\mu dN \qquad [A2]$$

where μ is the effective coefficient of friction. The frictional torque applied to the annulus at any point can then be calculated by the equation

$$dT_c=rdf \qquad [A3]$$

where dT_c is the frictional torque applied and r is the distance from the annulus rotational axis to any point. Then by substituting Eqs. [A1] and [A2] and the relation $dA= rdrd\theta$ into Eq. [A3] the following is obtained:

$$dT_c =r\mu Prdrd\theta \qquad [A4]$$

The pressure, P, is easily calculated by dividing the total load on the annulus by the area of the annulus or

$$P= F_a/[\pi(r_o^2-r_i^2)] \qquad [A5]$$

Next Eq. [A4] is integrated to get T_c, the frictional torque, as follows

$$T_c = \int_{r_i}^{r_o}\int_{0}^{2\pi} r^2 \mu P dr d\theta = 2\pi\mu P\left(r_o^3 - r_i^3\right) \qquad [A6]$$

Now substituting in Eq. [A5] for P provides

$$T_c = \frac{2}{3}\mu F_a \frac{r_o^3 - r_i^3}{r_o^2 - r_i^2} \qquad [A7]$$

Then solving for μ, Eq. [2] is obtained.